Planet. Space Sci., Vol. 39, No. 4, pp. 627–639, 1991
Printed in Great Britain.

0032-0633/91 $3.00+0.00
© 1991 Pergamon Press plc

A COMPARISON OF MEASUREMENTS OF THE OXYGEN NIGHTGLOW AND ATOMIC OXYGEN IN THE LOWER THERMOSPHERE

DAVID E. SISKIND and WILLIAM E. SHARP
Space Physics Research Laboratory, University of Michigan, Ann Arbor, MI 48109, U.S.A.

(*Received in final form* 1 *October* 1990)

Abstract—We have investigated the relationship between the oxygen nightglow and the atomic oxygen density in the lower thermosphere. This was done using data from two sounding rocket experiments conducted over White Sands Missile Range (32°N, 106°W). The first flight was launched on 2 November 1978 while the second was launched on 7 December 1981. Both flights contained resonance lamps to measure the atomic oxygen density. The peak density in both cases was near 1.9×10^{11} cm^{-3}. In addition, the 1978 flight contained a photometer to measure the 5577 Å green line while the 1981 flight contained photometers to measure the green line, the u.v. nightglow, and the 7620 Å (0,0) atmospheric band. We have used empirical models of these airglow features to compare with the O density measurements. In the case of the atmospheric band, excellent agreement is seen concerning the shape of the atomic oxygen profile, while some discrepancies were seen with the Herzberg band and the green line. In all cases, the absolute value of our peak O density appeared to be about 2.5 times lower, for a given airglow intensity, than previous measurements.

INTRODUCTION

Two of the fundamental problems in aeronomy are the measurement of atomic oxygen densities in the upper mesosphere and lower thermosphere and the relationship between atomic oxygen and the airglow in the 90–100 km region. The first paper of this series (Sharp, 1991, this issue, hereafter Paper 1) discussed the difficulties associated with measuring atomic oxygen from sounding rockets and presented the results from a number of rocket experiments. Even once these difficulties are resolved, however, rocket measurements are inherently limited in that they can only provide a local, instantaneous measurement. Furthermore, due to the relative inaccessibility of the 100 km altitude region to both balloons and satellites, the only viable approach to obtaining O densities on a global scale is through the remote sensing of airglow. Unfortunately, many of the details concerning the production of the lower thermospheric airglow remain incompletely understood. For example, people have historically used measurements of the 5577 Å green line to deduce O densities since the green line is so bright and thus easy to measure (Donahue *et al.*, 1973; Wasser and Donahue, 1979; Cogger *et al.*, 1981). Unfortunately, recent results suggest that an unidentified precursor is involved in the production of the green line (Bates, 1988b; Thomas, 1981) as well as the 7620 Å (0,0) atmospheric band which has also been used as a monitor of atomic oxygen (Murtagh *et al.*, 1990; McDade *et al.*, 1986a). This may complicate the extraction of [O] densities from measurements of these airglow features. Alternatively, while it is now thought that the O_2 ($A^3\Sigma_u^+ - X^3\Sigma_g^-$) Herzberg I emission is produced from direct three-body recombination, this emission is much weaker than the green line or the atmospheric band and is characterized by a vibrational distribution which is not yet completely explained (Siskind and Sharp, 1990; Stegman *et al.*, 1989; McDade *et al.*, 1982).

Despite these uncertainties, there have been a number of advances made recently in our understanding of the oxygen airglow. A set of simultaneous oxygen density and oxygen airglow observations was performed as part of the ETON rocket campaign (Greer *et al.*, 1986). Using these observations, a number of empirical airglow models have been developed (Murtagh *et al.*, 1986; McDade *et al.*, 1986a). A distinguishing feature of these models is that, in the case of the green line and the atmospheric band, they allow intensities to be calculated without a knowledge of the identity of the precursor. Murtagh *et al.* (1990) have shown that these models can be used to predict the green line intensity in some cases where no atomic oxygen density measurement was available. What we will show in this paper is that these airglow models offer a means to relate an [O] measurement made in one set of circumstances to that measured at a different time.

In Paper 1, six rocket measurements of lower thermospheric atomic oxygen were presented. Two of these experiments occurred at midlatitudes after

TABLE 1. SUMMARY OF ROCKET FLIGHTS (ALL LAUNCHED FROM WHITE SANDS MISSILE RANGE, 32°N, 106°W)

Flight No.	Rocket No.	Launch date	Launch time	SZA	A_p	$F10.7$
1	13.135	2 Nov. 1978	18:21 LST	102°	10	152
2	4.339	7 Dec. 1981	18:00 LST	102°	15	287

sunset, and were accompanied by a measurement of at least one oxygen nightglow feature. In this paper, we will use the airglow profiles in conjunction with the empirical models mentioned above to derive oxygen atom profiles. These profiles will then be compared with the measurements of Paper 1. Our goals are (1) to assess the validity of the O profiles given in Paper 1, (2) to compare them, at least indirectly, against other similar measurements, and (3) to see how well the atomic oxygen profile can be inferred from airglow.

EXPERIMENTAL DATA

The data to be discussed in this paper are taken from two rocket experiments which are summarized in Table 1. These rockets were both launched from WSMR about 1 h after sunset during quiet geomagnetic conditions and moderate-to-high solar activity levels. For purposes of clarity, for the rest of this paper, NASA flight 13.135 (the 1978 rocket) will be referred to as Flight 1 and NASA flight 4.339 (the 1981 rocket) will be referred to as Flight 2.

In addition to the [O] measurements presented in Paper 1, these rocket payloads contained a variety of other mesospheric and thermospheric experiments, some of which have been discussed in previous papers. Thus, Rusch and Sharp (1981) described a study of thermospheric odd nitrogen using data from Flight 1, while Sharp and Kita (1987) presented a measurement of atomic hydrogen from Flight 2. Here, we are most interested in the observations of the 5577 Å (O^1S–O^1D) green line, O_2 ($A^3\Sigma_u^+$–$X^3\Sigma_g^-$) Herzberg I bands, and the 7620 Å (0,0) $O_2(b^1\Sigma_g^+$–$X^3\Sigma_g^-)$ atmospheric band. All three of these emissions are believed to result, either directly or indirectly, from the three-body recombination of atomic oxygen and thus can be used to compare with our [O] measurements. A summary of the specific experiments used in this paper is given in Table 2.

As shown in the table, the green line was measured on both Flights 1 and 2, while Flight 2 also included measurements of the Herzberg nightglow and the (0,0) atmospheric band. Also indicated in the table is a measurement of the NO_2 continuum. This emission is believed to be due to the recombination of NO and O (McDade *et al.*, 1986b); here, however, this photometer channel will be most useful as an indicator of possible background contamination. The rest of this section is divided into subsections which describe in greater detail our measurements of [O], the atmospheric band, the Herzberg I bands and the green line.

Atomic oxygen density measurements

The two atomic oxygen profiles which will be analyzed in this paper are shown in Fig. 1. Panel (a) presents the Flight 1 data, while panel (b) shows the Flight 2 data. Data were typically obtained every 0.4 s, corresponding to an initial altitude resolution of 0.2–0.3 km; however, for convenience in performing calculations, the data were placed on a 1 km grid. Also shown are the predictions given by the MSIS-86 empirical model (Hedin, 1987). The peak [O] and the total column O between 86 and 110 km for these four profiles are summarized in Table 3. A comparison of our data with MSIS reveals many differences, some of which were discussed in Paper 1. Specifically, our data are about a factor of 2.5 lower in peak magnitude and 3–5 km lower in peak altitude than MSIS. Also the MSIS profiles predict about 16% less column O for Flight 1 than for Flight 2, while the measured O indicates about 5% more O for Flight 1 than Flight 2.

TABLE 2. DESCRIPTION OF PHOTOMETER EXPERIMENTS

Feature	Wavelength (Å)	$\Delta\lambda$ (Å)	Sens. (Hz R^{-1})	Flight No.
O_2 Hrz I (4,4)	3141	42	150	2
$O(^1S)$	5577	12.2	55	2
		6.9	4.56×10^{-12} A R^{-1}	1
NO_2 continuum	5760	40	40	2
$O_2(b^1\Sigma_g^+)$	7620	32	0.14	2

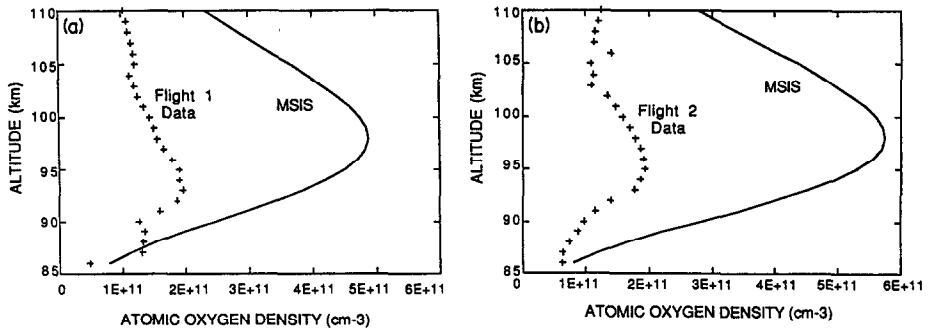

FIG. 1. MEASURED ATOMIC OXYGEN PROFILES FROM RESONANCE LAMP EXPERIMENTS ON FLIGHTS 1 [PANEL (a)] AND 2 [PANEL (b)].
Also shown are the MSIS-86 model predictions.

While these differences are small, since the nightglow typically depends upon $[O]^2$, it would be expected to respond noticeably to such small changes. For the rest of this paper, we will use the airglow measurements as a means of evaluating the different O profiles shown in Fig. 1.

7620 Å atmospheric band measurements

The 7620 Å (0,0) atmospheric band was measured on Flight 2 by a photometer which viewed the emission along the direction of the rocket trajectory. Only upleg data were obtained because of scattered moonlight on the downleg. The calibration of the photometer is given in Table 2. One problem with this calibration was that a large decrease in sensitivity was noted after it was integrated onto the payload. The cause of this change is not clear but we believe it may be the result of a problem in the telemetry system of the payload. Although the photometer calibration was remeasured while it was on the payload, the decreased sensitivity made it more difficult to calibrate accurately. As a result, a relatively large systematic uncertainty (on the order of 50%) is associated with the absolute intensity of the 7620 Å measurement. The transmission function of the filter was measured before the flight and convolved with a synthetic spectrum of the (0,0) atmospheric band provided to us by J. H. Yee (private communication, 1990). The transmission of the filter was approx. 30% assuming a rotational temperature of 200 K.

The resulting 7620 Å column intensity profile is shown in Fig. 2a. The dotted line is the raw data, binned in 1/2 km increments, while the solid line is the smooth fit. Smoothing the data is necessary because the calculation of volume emission rates involves differentiation of the column intensities and this process greatly amplifies any noise that is present. A number of filtering and differentiation techniques have been discussed (Murtagh *et al.*, 1984; Kita *et al.*, 1989); however, all of them involve a degree of subjectivity, either in the amount of filtering that is applied, or in the assessment of the resultant errors. We used two techniques: the incremental straight line fitting approach of Thomas and Young (1981) and Fourier filtering. As shown by Murtagh *et al.* (1984), the first technique appears to more accurately reproduce the small-scale structure present in their test profiles; however, we found Fourier filtering more useful for especially noisy profiles and more convenient in quantifying the errors associated with differentiating the zenith radiance profiles. The low pass filter used for the 7620 Å profile had a cut-off such that all frequencies higher than 6 km $cycle^{-1}$ were removed. Our error analysis is discussed in the appendix. Figure 2b shows the resulting 7620 Å volume emission rate profile.

TABLE 3. SUMMARY OF ATOMIC OXYGEN PROFILES

Flight	Measured peak [O] (cm^{-3})	MSIS peak [O] (cm^{-3})	Measured column* (cm^{-2})	MSIS column* (cm^{-2})
1	1.95×10^{11}	4.87×10^{11}	3.45×10^{17}	8.58×10^{17}
2	1.92×10^{11}	5.75×10^{11}	3.29×10^{17}	1.01×10^{18}

*Total column between 86 and 110 km.

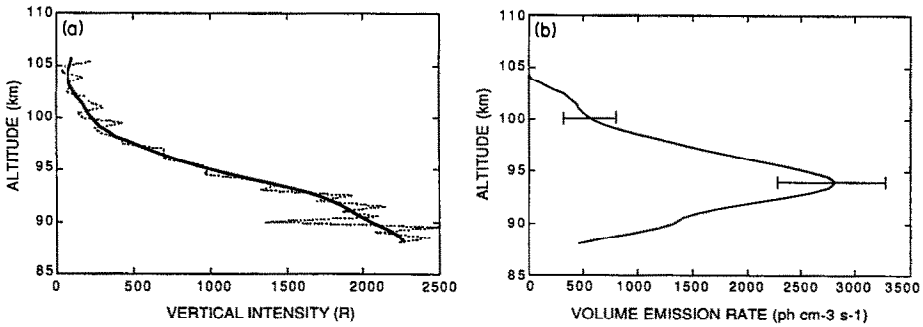

FIG. 2. THE 7620 Å (0,0) ATMOSPHERIC BAND OBSERVATION FROM FLIGHT 2.
Panel (a) shows the zenith intensity profile. The dotted lines are the data binned every 0.5 km and the solid line is the result of applying a low pass Fourier filter. Panel (b) shows the volume emission rate profile obtained by differentiating the solid curve in panel (a).

Herzberg I measurement

The u.v. nightglow was monitored on Flight 2 by a single channel photometer with a bandpass centered at 3158 Å. Our model of the various nightglow emissions likely to be present in the photometer bandpass, using the synthetic spectrum code of Sharp and Siskind (1989), indicates that the largest contribution to the observed signal comes from the O_2 Herzberg I (4,4) band which has a band origin near 3141 Å. The exact fraction, however, contains some uncertainty and thus merits some discussion. Using the Sharp and Siskind (1989) data as a guide, we find that approx. 68% of the observed signal comes from the (4,4) band, 15% comes from other Herzberg I bands such as the (2,3) and (3,4) bands, 15% comes from the Herzberg II (5,3) and (3,2) bands and the remainder from several weaker bands including the Chamberlain (8,0) band. On the other hand, Stegman and Murtagh (1991) suggest that there should be more Herzberg II emission, particularly from high v' levels (up to 11), than seen by Sharp and Siskind (1989). In addition, there was a u.v. limb scanning spectrometer on Flight 2 which observed the nightglow from 3000 to 3400 Å. Unfortunately, it appears that during the limb scanning phase of the experiment, the rocket was pointing below the airglow layer peak. As a result, we cannot quantify any possible altitude variation in the nightglow spectra from these data; however, a preliminary analysis of these data using synthetic spectra does suggest a larger Herzberg II emission on Flight 2 than seen by Sharp and Siskind (1989). In this case, we find the Herzberg I (4,4) band contribution to our photometer signal could be as low as 52% of the total, while the Herzberg II contribution would increase to 33%. This may then introduce a second uncertainty, namely the possibility that the Herzberg II has a different altitude profile than the Herzberg I which would confuse an analysis of the photometer intensity profile. As we will discuss, however, this second uncertainty would have little effect on our conclusions. Therefore as a compromise between the range of values discussed above, we multiplied the photometer intensity by a fixed value of 0.6 and assumed it represented the signal from the Herzberg I (4,4) band. The implications of this assumption will be considered in a later section.

Figure 3a shows the resulting Herzberg I (4,4) profile derived in the above manner. This profile was obtained with the photometer viewing the zenith on the upleg portion of the flight. As was the case with the 7620 Å measurement on this flight, no data were obtained on the downleg. The figure shows the raw data (dotted curve) as well as the data after Fourier filtering (heavy solid curve). The filtering was of the same degree as with the 7620 Å profile. Also shown is our estimate of the background intensity. There is a small uncertainty in this estimate because the rocket began a limb scanning maneuver at 105 km and some residual Herzberg emission above this altitude is still possible. Our background estimate shown in the figure attempts to account for this. The difference between this background and the emission measured below 90 km yields an intensity estimate for the (4,4) band of 13.9 ± 3.5 R. The estimated error includes a calibration error (15%), background subtraction (10%), counting statistics for a 0.5 km data bin (10%) and our estimate of the error in evaluating the contribution of the (4,4) band to the total signal (15%). To convert to a total Herzberg system intensity, we need to make an assumption about the fraction of total emission contained in this single band. Using Degen's (1977) table, we find that 5% of the total emission is in the

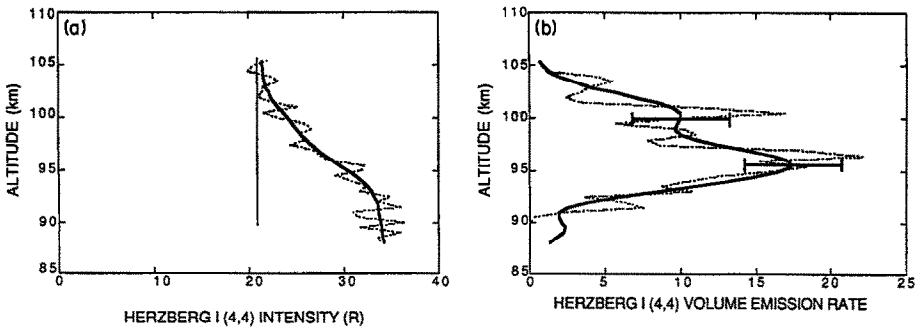

FIG. 3. (a) ZENITH INTENSITY OF THE HERZBERG I (4,4) BAND OBTAINED ON FLIGHT 2. The dotted line is the data binned every 0.5 km, the heavy solid line is the result of Fourier filtering and the vertical solid line is the background estimate. (b) Corresponding volume emission rate (VER). The solid line is the VER obtained after differentiation of the heavy solid curve in the (a). The dotted line is the VER obtained using a linear least-squares fitting routine (see text).

(4,4) band and the total system intensity becomes 278 ± 70 R. A similar value results using our published vibrational populations (Sharp and Siskind, 1989) and Bates' (1989) A-values. Unlike our model of the photometer signal, this value does not depend upon an uncertain ratio of Herzberg I to Herzberg II and thus the error associated with the extrapolation to a total Herzberg system intensity is smaller than the uncertainties discussed above.

The resulting volume emission rate profile is shown as the solid line in Fig. 3b. As with the 7620 Å profile, the error bars are discussed in the appendix. In addition, we present, as the dotted line, the result of using the straight line fitting technique with 5 km segments. A comparison of the two profiles gives a more qualitative indication of the uncertainty in the result and also provides some evidence for structure (or a secondary maximum) in the profile near 100 km.

5577 Å green line

The green line is one of the most commonly observed nightglow features since it is so bright and easily observed from the ground. We obtained a green line profile on the upleg portion of both Flights 1 and 2. For Flight 1, this emission was the only reliably measured oxygen emission. Figure 4 shows the volume emission rate profiles for both flights, calculated using Fourier filtering. Since the green line profiles contained less noise than either the Herzberg or atmospheric band profiles, the filtering required was less. The filter used contained a cut-off at 4.5 km. For Flight 1, the peak emission was 320 photons $cm^{-3}\ s^{-1}$ at 95 km, and for Flight 2, the peak emission was 150 photons $cm^{-3}\ s^{-1}$ at 96 km.

Note that while the green line of Flight 1 was twice as bright as on Flight 2, the measured O profiles

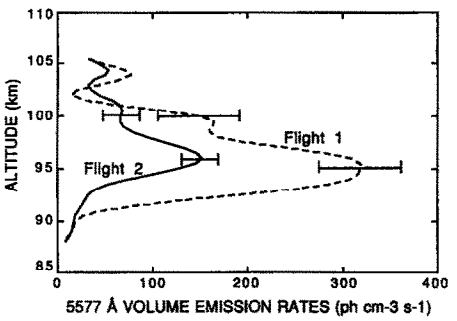

FIG. 4. VOLUME EMISSION RATE OF THE 5577 Å GREEN LINE OBTAINED FROM BOTH FLIGHTS.

showed little difference and the MSIS O profiles for this flight predicted the opposite trend. On the other hand, as Stegman and Murtagh (1988) and Murtagh *et al.* (1990) have recently shown, the green line intensity can vary from 30 to 400 R; thus, both of our profiles fall within the range of previous observations. The profile on Flight 2 peaks at the same altitude as the Herzberg profile and 1.5 km higher than the atmospheric band profile measured on the same flight; again, this is similar to previous observations (Greer *et al.*, 1986). Also, the fact that the peak altitude on Flight 1 is 1 km lower than on Flight 2 appears qualitatively consistent with the [O] measurements which showed a lower O layer on Flight 1. Finally, it is of interest to note that both green line profiles show a similar "bump" at 99–101 km as did the Herzberg profile on Flight 2.

Table 4 summarizes the observed column intensities for both green line observations as well as the Herzberg and atmospheric band observations on Flight 2.

TABLE 4. SUMMARY OF AIRGLOW OBSERVATIONS*

Feature	Flight 1	Flight 2
Herzberg I	—	278±70 R
7620 Å atm band	—	2.3±1.2 kR
5577 Å green line	235±33 R	105±15 R
5760 Å NO_2 continuum		See text

* Average of upleg and downleg column intensities.

ANALYSIS

In this section, we attempt to fit our measured airglow profiles using our measured [O]. Typically, in the past people have used such simultaneous [O]/airglow measurements to derive quenching rates and excitation efficiencies (e.g. McDade *et al.*, 1986a; Thomas, 1981; Thomas *et al.*, 1979). Since the derived kinetic parameters have tended to differ with each experiment, it makes intercomparisons between experiments difficult. Therefore, rather than simply repeating the earlier analyses, we will adopt previously derived airglow models (largely those from the ETON campaign) and test them against our data. Since these models have had some success in characterizing the airglow, we suggest that they can serve as a common basis for comparing different measurements of the atomic oxygen density. This section is thus divided into three subsections: the first summarizes the airglow models, while the second and third apply them to the two sets of rocket data (Flights 1 and 2) using our measured [O].

Empirical airglow models

The models we use for the atmospheric band and the green line were first developed by McDade *et al.* (1986a) and have been recently used by Murtagh *et al.* (1990). As they discuss, it is possible to parameterize the volume emission rate of the atmospheric band in terms of the atomic oxygen density and the as yet unidentified precursor of the $O_2(b^1\Sigma_g^+)$. The expression they give is

$$V_{atm} = \frac{A_1 k_1 [O]^2 \{[N_2]+[O_2]\}[O_2]}{\{A_2+k_2^{O_2}[O_2]+k_2^{N_2}[N_2]+k_2^{O}[O]\}\{C^{O_2}[O_2]+C^{O}[O]\}}, \quad (1)$$

where A_1 is the (0,0) band transition probability, A_2 is the inverse radiative lifetime of $O_2(b^1\Sigma_g^+)$, k_1 is the rate coefficient for three-body recombination of atomic oxygen, k_2 are the rate coefficients for quenching of $O_2(b^1\Sigma_g^+)$ by atmospheric O_2, N_2 and O, and C^{O_2} and C^{O} are related to the excitation and quenching (by O_2 and O) of the unidentified O_2 $(b^1\Sigma_g^+)$ precursor. Both McDade *et al.* (1986a) and Murtagh *et al.* (1990) use a variety of values for C^{O_2} and C^{O}, depending upon the neutral atmosphere they adopted and the assumed rate of quenching of $O_2(b^1\Sigma_g^+)$ by atomic oxygen. Once these assumptions are made, equation (1) can be expressed as a quadratic equation for [O] and readily solved.

For the green line, the parameterization for the volume emission rate is

$$V_{O(^1S)} = \frac{A_5 k_1 [O]^3 \{[N_2]+[O_2]\}}{\{A_6+k_5[O_2]\}\{C'^{O_2}[O_2]+C'^{O}[O]\}}, \quad (2)$$

where A_5 is the $O(^1S–^1D)$ transition probability, A_6 is the inverse $O(^1S)$ radiative lifetime, k_5 is the coefficient for quenching of $O(^1S)$ by O_2, and C'^{O_2} and C'^{O} relate to the unidentified $O(^1S)$ precursor. Values for all these parameters were taken from Table 1 of Murtagh *et al.* (1990). Values for the number densities of N_2, O_2 and the temperature T were taken from the MSIS-86 empirical model. In this case, we get a cubic equation for the atomic oxygen density.

Finally, for the Herzberg bands, we assumed that the emission results from direct three-body recombination of O, rather than through a precursor (e.g. Siskind and Sharp, 1990; Murtagh *et al.*, 1986). In the simplest case, where we assume that the vibrational distribution is invariant with altitude, the volume emission rate is expressed as

$$V_{Hrzl} = \frac{A_H \varepsilon k_1 [O]^2 \{[N_2]+[O_2]\}}{A_H + k_E[O_2]}, \quad (3)$$

where A_H is the total $O_2(A^3\Sigma_u^+)$ inverse lifetime, ε is the fractional recombination yield of $O_2(A^3\Sigma_u^+)$, and k_E is the electronic quenching rate coefficient. Here, it is assumed that the dominant quencher is O_2 and for a given value of k_E and ε, it is straightforward to derive an O profile from a given measurement of V_{Hrzl}. Unfortunately, as we have shown previously (Siskind and Sharp, 1990) the vibrational distribution does depend somewhat upon altitude and this complicates the situation. In this case, the emission in a given band can no longer be expressed as simply as in equation (3); rather, it must be calculated using a model which accounts for vibrational relaxation. We discussed several of these models in the above referenced paper and showed that the nightglow spectra could be best fit if the electronic quenching, k_E, lay between 3×10^{12} cm^3 s^{-1} (intermediate quenching–hereafter called Model A) and 1.5×10^{11} cm^3 s^{-1} (high quenching–hereafter called Model B). These quenching values are both higher than the values given by Kenner and Ogryzlo

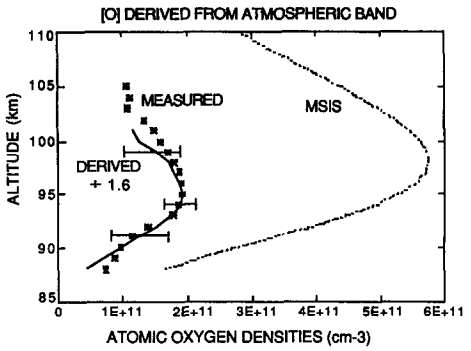

FIG. 5. COMPARISON OF THREE ATOMIC OXYGEN PROFILES FOR FLIGHT 2.
The stars are the direct measurement. The solid line is the [O] derived from the 7620 Å measurement and equation (1) in the text. The derived O has been divided by 1.6 to fit the absolute magnitude of the measured O (see text). The dotted line is from the MSIS model.

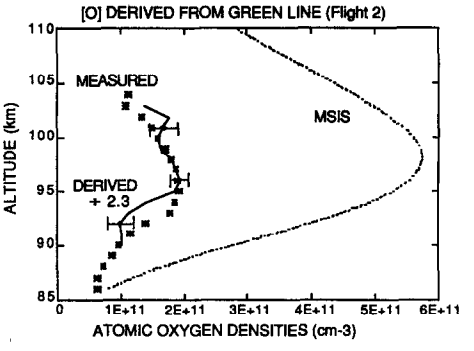

FIG. 6. SAME AS FIG. 5 EXCEPT THE SOLID LINE IS THE [O] DERIVED FROM THE 5577 Å GREEN LINE MEASUREMENT AND EQUATION (2) IN THE TEXT.
Here, the derived O has been divided by a scaling factor of 2.3.

(1980, 1983, 1984). In both these models, the emission rate is still linearly dependent upon the product of ε and $[O]^2$ and thus a fit to a measured airglow profile can yield a value for this quantity. Furthermore, Model B is essentially the same as that derived by Murtagh *et al.* (1986) from ETON data with $\varepsilon = 0.04$. We can thus use our Herzberg I measurement to independently check the derived O densities obtained from the atmospheric band and green line profile and compare our results with previous ones.

Analysis of Flight 2 data

Since Flight 2 contained the most comprehensive set of photometer measurements, we will discuss it first. The results from our 7620 Å measurement are shown in Fig. 5. The figure presents three O profiles, one from MSIS, our direct measurement, and a derived O profile obtained from the solution of equation (1). The derived O profile was calculated using $k_2^O = 8 \times 10^{-14}$ cm^3 s^{-1} and respective values for C^{O_2} and C^O equalling 6.6 and 19 (see Murtagh *et al.*, 1990). It also has been scaled downwards by a factor of 1.6 to best fit the measurement. This scaling factor may reflect a discrepancy in the absolute calibration between our [O] measurement and that used in the ETON analysis. As Murtagh *et al.* (1990) point out, if the ETON O densities were in error by some constant factor α, the O densities derived from their parameterization would also be in error by α. [This is strictly true only with no O quenching of $O_2(b^1\Sigma_g^+)$; however for our [O] values, the effect of O quenching was less than 5% on the derived O.] With this in mind, it is nonetheless clear that there is an excellent agreement in the shapes of the two curves. Such agreement is encouraging, especially when one considers that the fit is sensitive to the ETON O measurement, the ETON 7620 Å data (and model), our 7620 Å data and our O measurement. Furthermore, it is clear from the figure that the atomic oxygen profiles deduced from either direct measurement or from the 7620 Å measurement agree much more closely with each other than either does with MSIS.

Given the relatively large uncertainty in the absolute calibration of the 7620 Å photometer, it is important to look at the [O] derived from the other two airglow profiles. Figure 6 shows the derived atomic oxygen profile using our green line measurement in equation (2) and compares it with our direct measurement and MSIS. The figure shows that, as with the 7620 Å profile, the derived and measured O profiles agree with each other more closely than either does with MSIS. For example the MSIS O shows a peak at 98 km, while the two other curves both peak around 95–96 km. There are, however, some greater discrepancies between the shapes of the derived and measured O profiles than is seen in Fig. 5. In particular, the derived curve shows about 30% less atomic oxygen between 91 and 94 km than the measurement. Also since the green line emission extends about 3 km higher than the 7620 Å emission, we note a significant enhancement in the derived O profile at 101 km that is not seen in the measurement. Also, the derived [O] was scaled downwards by a factor of 2.3 to produce the best fit with the data. Thus both the atmospheric band data and the green line data suggest that for a given airglow intensity, our measured atomic oxygen density is less than that of ETON.

Finally, Fig. 7 shows the results of comparing our measured Herzberg profile with that calculated using

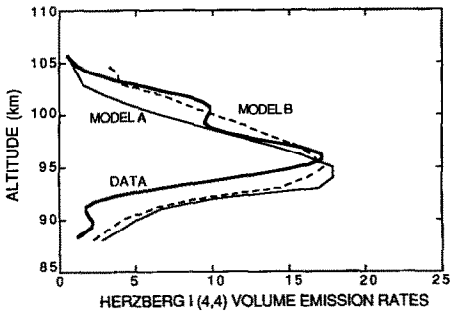

FIG. 7. HERZBERG (4,4) PROFILE COMPARED WITH THEORETICAL CALCULATION.
The lighter solid line is model A (intermediate quenching) with an excitation efficiency of 5%. The dashed line is model B (high quenching) with an excitation efficiency of 23%.

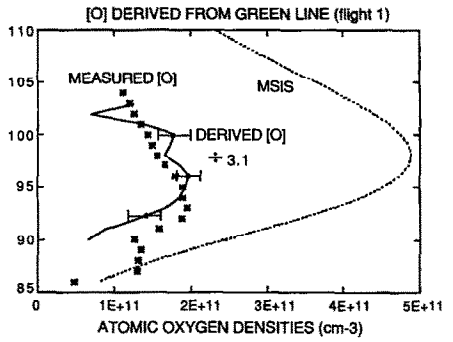

FIG. 8. COMPARISON OF THREE ATOMIC OXYGEN PROFILES FOR FLIGHT 1.
The format is similar to Figs 5 and 6. The derived O is obtained from a simultaneous 5577 Å green line measurement and equation (2) in the text. The derived O has been divided by 3.1 in order to fit the absolute magnitude of the measured O.

the two quenching models described above. In this case, rather than presenting a derived [O] density profile, we are showing the results of a more conventional "forward" calculation of the airglow intensity. The figure shows that both models do a fair job of reproducing the data; however, there are a number of discrepancies which are similar to that seen in the green line analysis. First, the calculated emission significantly exceeds the observation from 91 to 94 km. Second, the calculated emission does not reproduce the secondary maximum at 101 km. This is analogous to what was shown in Fig. 6, where the airglow suggests that more O should be present at 100–101 km and less O between 91 and 94 km than is actually observed. This will be discussed further in a later section. For now, we are more interested in the production efficiency, ε, required to match the observed peak emission rates. For Model A, we require $\varepsilon = 0.05$ while Model B, with its higher loss due to quenching, requires $\varepsilon = 0.23$. This second value is almost $6\times$ greater than that used by Murtagh *et al.* (1986) for similar quenching coefficients. A likely explanation for this difference is that for a given Herzberg intensity, our [O] is lower than that reported by Greer *et al.* (1986). Since ε varies inversely as $[O]^2$, a $6\times$ greater value of ε is equivalent to an oxygen density which is lower by a factor of 2.4. This agrees well with the factor of 2.3 which we inferred from the green line data. It is greater than the 1.6 scaling derived from the atmospheric band; however, given the calibration uncertainty associated with that measurement, we feel our absolute Herzberg band and green line intensities are more reliable. Also note that due to the quadratic relationship between ε and [O], even a 20% error in our estimate of the Herzberg I (4,4) contribution to the photometer signal would only result in a 10% error in our estimate of this scaling factor. Thus we conclude that for a given level of airglow intensity, the atomic oxygen measurement on Flight 2 is lower than that of Greer *et al.* (1986) by about a factor of 2.4.

Analysis of Flight 1 data

As we have already mentioned, the only airglow profile obtained on Flight 1 was the 5577 Å green line. We have used our measured profile in conjunction with equation (2) to derive an [O] profile. The results are shown in Fig. 8 which compares [O] profiles from MSIS, the green line and from the resonance lamp experiment. The figure shows that the derived and measured profiles have similar shapes, particularly in their top side scale heights; however, there is a discrepancy in the peak altitude. Thus the derived profile (which reflects the height of the airglow layer) peaks in the range 95–97 km, while the measured O shows a peak between 92 and 95 km. Compared with Flight 2, both the derived and measured profiles are at a lower altitude while the MSIS profiles predict little change. Below the peak of the measured O, the inferred O is consistently lower in magnitude, a behavior which is qualitatively similar to that seen on Flight 2. We will argue below that the discrepancies seen on the two flights may both be related to rocket glow.

Concerning the absolute value of the derived O density peak shown in Fig. 8, it was divided by 3.1 to match the peak atomic oxygen measured by the resonance lamp. This means that the ETON model, which we used, is normalized to an O density that is $3.1\times$ greater than what we measured. This is a greater scaling factor than was derived from the Flight 2

data and reflects the fact that the green line intensity measured on Flight 1 was about twice as bright as that observed on Flight 2, while the measured O showed only a small change. While this at first glance suggests some inconsistencies with our data, it actually falls within the calibration uncertainty of the O measurement. This is because for the values of O near 2×10^{11} cm^{-3}, the green intensity as given by equation (2) exhibits a nearly cubic dependence upon the O density. As a result, a 30% change in O can lead to a factor of 2 change in the green line emission. Thus, our two measurements can be made consistent if the measured O on Flight 1 were too low by 30% while that on Flight 2 were too high by a similar amount. Given the estimated uncertainty of 30% associated with an individual measurement of atomic oxygen (see Paper 1), it is not unreasonable to suggest that two separate measurements could differ by 60%. In fact, this 60% disagreement, while certainly not insignificant, compares favorably with the factors of 2–10 discrepancies reported by Murtagh *et al.* (1990) and Dickinson *et al.* (1987) for similar sets of observations. It does, however, point out the importance of combining a given measurement of O with a simultaneous measurement of at least one airglow indicator.

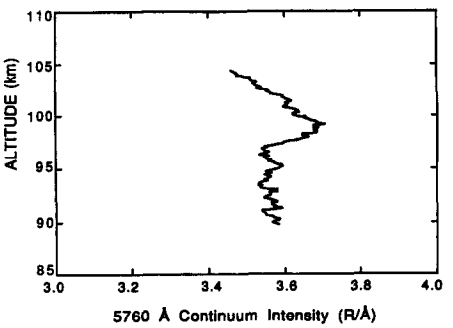

FIG. 9. COLUMN INTENSITY OF 5760 Å CONTINUUM FOR FLIGHT 2.

DISCUSSION

In the previous section, we saw some differences between the O profile inferred from airglow with the O measured by the resonance lamp. For the two green line profiles and the Herzberg profile on Flight 2, the models generally indicate significantly less O than the data below the peak of the layer. An alternate (and equivalent) way of stating this is that the observed airglow cuts off more sharply than the model below the layer peak. This is particularly evident in our Herzberg profile (Fig. 7). A discrepancy of this sort is difficult to explain because it necessitates a loss mechanism which increases at lower altitudes more rapidly than the rapid molecular quenching already included in the model. It is important to note here that the presence of significant Herzberg II in the u.v. photometer data would only make the discrepancy worse. This is because it is thought that the $c^1\Sigma_u^-$ state is quenched by O (e.g. McDade *et al.*, 1984) which would lead to a Herzberg II layer several kilometers below the Herzberg I. If there is an unaccounted for Herzberg II emission in our data, the "missing" emission below 95 km becomes even more glaring. In addition, when one considers that the excitation mechanisms for the green line and the Herzberg bands are assumed to be different, it becomes more difficult to ascribe these discrepancies to simple model error. Finally, it might be argued that this suggests a problem with the O measurement; however, at least on Flight 2, this is precluded by the fit to the O derived from the 7620 Å data (Fig. 5). Therefore, one possibility that we will explore in this section is that these discrepancies may result from a transient rocket-induced glow.

Support for the existence of rocket glow is seen in Fig. 9 which presents the observed zenith intensity (including the sky background) from the 5760 Å photometer. Normally, one would expect to see the emission decrease from 95 to 100 km as the rocket passed through the NO_2 continuum layer (McDade *et al.*, 1986b; Witt *et al.*, 1981). Instead we see a noticeable *increase* in the signal, centered around 99 km. This is inconsistent with what one would expect in an airglow measurement but seems to coincide with the high altitude "bumps" seen in the Herzberg band and green line profiles on the same flight. Given that the onboard magnetometers indicate no change (to within $\pm 0.1°$) in rocket attitude and thus no change in the background during this time frame, an induced glow becomes the most likely explanation. The intensity of the enhancement seen in the figure is 0.125 R Å^{-1}; however, the actual contamination is most likely much greater than this. This is because a typical brightness for the NO_2 layer is of the order of 0.4 R Å^{-1} (McDade *et al.*, 1986b; Gadsen and Marovich, 1973). In order for the NO_2 emission to be completely obscured (as it is in Fig. 9), the rocket glow would have to be at least 0.5 R Å^{-1}.

The existence of a rocket glow phenomenon has been reported in the past. In some cases (Witt *et al.*, 1984; Lopez-Moreno *et al.*, 1985), the contamination is clearly evident due to an increase in the signal as the rocket passes through the airglow layer; in others (McDade *et al.*, 1987a,b), the presence of contamination has been invoked to explain differences

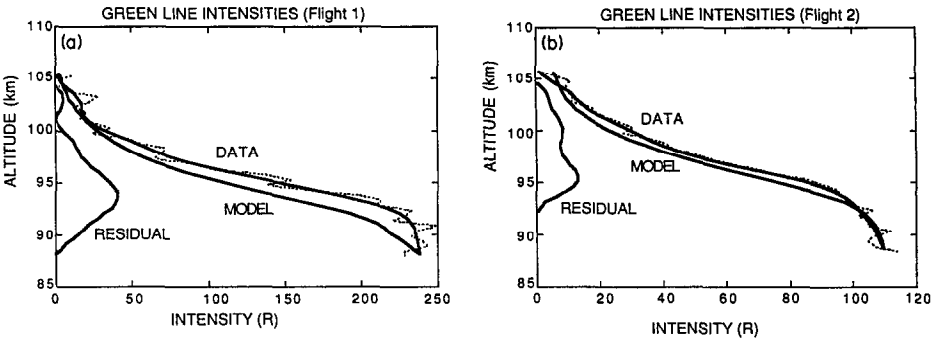

FIG. 10. COMPARISON OF 5577 Å ZENITH INTENSITY PROFILES.
Panel (a) is for Flight 1; panel (b) is for Flight 2. The model profiles were calculated using equation (2) in the text and have been normalized to the data at the base of the layer. The difference between the measured and model profiles is shown as a residual emission.

between models and observations. McDade *et al.* (1987a) discussed the effect that "hidden" contamination would have on a zenith intensity measurement. If the contamination is increasing with increasing rocket altitude, the measured zenith profile will decrease more slowly with height and the volume emission will be underestimated. Conversely, the inferred volume emission will be too large if the contamination is decreasing with increasing altitude. In order to quantitatively assess these effects, we have followed the approach used in the two McDade *et al.* papers. In those papers, they calculated the residual difference between their observed column intensity profiles and their models.

Two samples of such a calculation are shown in Fig. 10a and b for the two green line profiles. The data in the figure are the observed zenith intensity with an apogee background subtracted. The model is the result of using the measured [O] (scaled as discussed in the previous section) in equation (2), with a small additional normalization (of about 15%), so that the two curves agree below the layer. In this manner, we can highlight the differences in shape between the measurements and the models. It is apparent in both panels that the model profiles start decreasing at a lower altitude than do the data. The residual difference, or excess intensity, peaks at 93 km for Flight 1 and 95 km for Flight 2. The magnitude of this excess is about 50 R (or 17 R $Å^{-1}$) for Flight 1 and about 10 R (or 1.7 R $Å^{-1}$) for Flight 2.

The shapes and magnitudes of our derived residual intensity profiles are generally consistent with those reported previously. The deduced intensities are such that the weaker Herzberg band and green line measurements would be more sensitive to such contamination than the stronger 7620 Å emission, in agreement with our observation. On the other hand, our estimate of 1.7 R $Å^{-1}$ for Flight 2 is greater than the 0.5 R $Å^{-1}$ we estimated from the 5760 Å profile. In fact, subtracting the 5760 Å intensity from the 5577 Å data made no significant difference in the derived green line volume emission rate profile. This suggests that if there is a contaminating emission, it may not be a smoothly varying continuum.

In light of the above uncertainties, this hypothesis must still be considered speculative; however, given our lack of understanding about rocket–atmosphere interactions, it would be premature to rule out this possibility. It is interesting to note that Thomas (1981) also saw a discrepancy between his measured and modeled green line which is very similar to ours. In a subsequent analysis of the 1.27 μm emission from the same rocket flight, McDade *et al.* (1987a) proposed the presence of a contaminating emission. It may be that Thomas' 5577 Å data were also affected.

CONCLUSIONS AND CONSEQUENCES

In this paper we have used sets of simultaneous [O]/airglow measurements to investigate the relationship between the airglow and the atomic oxygen at lower thermospheric altitudes. Of particular interest was whether our data were consistent with previous measurements. For this analysis we conclude the following:

(1) The shape and peak altitude of the atomic oxygen layer is well characterized by the measurement technique of Sharp (1991, Paper 1). This is primarily based upon the agreement between the O derived from the atmospheric band profile on Flight 2 and that measured directly by the resonance lamp technique.

(2) For the two cases studied here, we found the O derived from the airglow was more consistent with measurement than it was with MSIS model predictions. The MSIS model predicted an O layer that was too high in altitude and that varied from Flight 1 to 2 in the opposite sense to both the airglow and the oxygen measurements. All this reinforces the point made most recently by Stegman and Murtagh (1988); namely, that it is pointless to discuss the variation of lower thermospheric atomic oxygen without some reference to an independent indicator such as airglow.

(3) By normalizing our measured atomic oxygen densities to a common reference airglow level, we find that the absolute magnitude of the O densities studied here is lower than that measured by Greer *et al.* (1986) during the ETON campaign. Using the ETON-derived airglow models, the difference between our O densities and ETON's ranges from 2.3 to 3.1

(4) The 7620 Å atmospheric band is well explained by the model of McDade *et al.* (1986a). No evidence was found for any additional source for this emission, provided the absolute magnitude of the [O] is scaled according to conclusion (3) above. The success of this model along with the brightness of the emission combine to make this feature an attractive monitor of O via remote sensing techniques.

(5) The 5577 Å green line and the Herzberg bands are only partially explained by the models used here. As we have suggested, this may be related to contamination of these data by a rocket-induced glow.

One obvious implication of these conclusions, specifically the third one, is that the peak O density may be lower than previously assumed. This, in turn, would have numerous consequences on the chemistry and energetics of the mesopause region (e.g. Brasseur and Offerman, 1986; Garcia and Solomon, 1985; Allen *et al.*, 1984). Consideration of these effects is beyond the scope of this paper, but there is one important point which must be addressed here. If the [O] is a factor of 2.5 lower than that of Greer *et al.* (1986), the processes which produce the observed airglow intensities must be correspondingly more efficient. For example, McDade *et al.* (1986a) state that $O_2(b^1\Sigma_g^+)$ must be formed in oxygen recombination with a minimum efficiency of 13%. With 2.5 times less atomic oxygen, the required efficiency increases to over 80%. While this seems high, we should note that since the excitation mechanism involves an energy transfer with O_2, efficiencies of over 100% are possible. Until the identity of the O_2 precursor is established, it will be difficult to assess the validity of a given value for the production efficiency of $O_2(b^1\Sigma_g^+)$.

In the case of the Herzberg bands, the situation is clouded by continuing uncertainties in the quenching rate coefficient for the O_2A state. With the ETON quenching coefficient (1.5×10^{-11} cm^3 s for O_2, using the higher Bates transition probabilities), our required efficiency is 23%. Recent theoretical estimates, as summarized by Bates (1988a), suggest a value of 6% for the percentage of recombinations which yield $A^3\Sigma_u^+$. This may indicate a problem with a Herzberg model that relies upon high quenching and low O. With our intermediate O_2 quenching value (3×10^{-12} cm^3 s^{-1}), we only required a production efficiency of 5%. Of course, neither of these quenching models exactly fit either our photometer data here or our spectrometer data discussed previously (Siskind and Sharp, 1990), so we cannot make a definitive statement about which model we prefer. An additional uncertainty is also discussed by Bates (1988a, 1989). He argues that the laboratory measured recombination rate (Campbell and Gray, 1973) does not include the production of $O_2(^5\Pi_g)$. This is because in the laboratory, $O_2(^5\Pi_g)$ will thermally redissociate and thus make no net contribution to the recombination. On the other, Bates points out that in the thermosphere, $O_2(^5\Pi_g)$ may be stable. Since it is thought that of the order of 50% of all recombinations enter into the $^5\Pi_g$ state, this means that the actual recombination could be up to twice what Campbell and Gray measured. Alternatively, if one uses the Campbell and Gray rate coefficient for thermospheric modelling, one would then have to double the production efficiency of a given state over theoretical values which include $^5\Pi_g$. In consideration of all these uncertainties, we conclude that while our lower O measurements require significant increases in the airglow production efficiencies, it would be premature to rule out such possibilities.

FINAL REMARKS

The ultimate question of which absolute value of O is the correct one still remains; however, it appears to be somewhat more constrained than previously. Our results suggest that there is an experimental discrepancy of about 2.5 between the technique used by Sharp (1991) and that used by Greer *et al.* (1986), but we cannot at this point determine which of the two is more accurate. It is interesting to note, however, that this discrepancy is much less than the factor of 10–40 discrepancy discussed by Llewellyn (1988), Sharp (1985), and Offerman *et al.* (1981). One possibility is that the more recent measurements of O are more accurate than many of the measurements summarized by Offermann *et al.* (1981). It is also likely that, guided by our increased understanding of the O_2 airglow, our

knowledge of the natural variability inherent in lower thermospheric atomic oxygen is also continuing to improve.

Acknowledgements—We thank I. C. McDade for helpful comments and suggestions. This research was supported by NASA Grant NGR23-005-360.

REFERENCES

Allen, M., Lunine, J. I. and Yung, Y. L. (1984) The vertical distribution of ozone in the mesosphere and lower thermosphere. *J. geophys. Res.* **89**, 4841.

Bates, D. R. (1988a) The excitation and quenching of the oxygen bands in the nightglow. *Planet. Space Sci.* **36**, 875.

Bates, D. R. (1988b) Excitation of 557.7-nm OI line in nightglow. *Planet. Space Sci.* **36**, 883.

Bates, D. R. (1989) Oxygen band system transition arrays. *Planet. Space Sci.* **37**, 881.

Brasseur, G. and Offerman, D. (1986) Recombination of atomic oxygen near the mesopause: interpretation of rocket data. *J. geophys. Res.* **91**, 10,818.

Campbell, I. M. and Gray, C. N. (1973) Rate constants for $O(^3P)$ recombination and association with $N(^4S)$. *Chem. Phys. Lett.* **18**, 607.

Cogger, L. L., Elphinstone, R. D. and Murphree, J. S. (1981) Temporal and latitudinal 5577 Å airglow variations. *Can. J. Phys.* **59**, 1296.

Degen, V. (1977) Nightglow emission rates in the O_2 Herzberg bands. *J. geophys. Res.* **82**, 2437.

Dickinson, P. H. G., Witt, G., Zuber, A., Murtagh, D. P., Grossmann, K. U., Bruckelmann, H. G., Schwabbauer, P., Baker, K. D., Ulwick, J. C. and Thomas, R. J. (1987) Measurements of odd oxygen in the polar region on 10 February 1984 during MAP/WINE. *J. atmos. terr. Phys.* **49**, 843.

Donahue, T. M., Guenther., B. and Thomas, R. J. (1973) Distribution of atomic oxygen in the upper atmosphere deduced from *Ogo* 6 airglow observations. *J. geophys. Res.* **78**, 6662.

Gadsen, M. and Marovich, E. (1973) The nightglow continuum. *J. atmos. terr. Phys.* **35**, 1601.

Garcia, R. R. and Solomon, S. (1985) The effect of breaking gravity waves on the dynamics and chemical composition of the mesosphere and lower thermosphere. *J. geophys. Res.* **90**, 3850.

Greer, R. G. H., Murtagh, D. P., McDade, I. C., Dickinson, P. H. G., Thomas, L., Jenkins, D. B., Stegman, J., Llewellyn, E. J., Witt, G., Mackinnon, D. J. and Williams, E. R. (1986) ETON 1: a data base pertinent to the study of energy transfer in the oxygen nightglow. *Planet. Space Sci.* **34**, 771.

Hedin, A. E. (1987) MSIS-86 thermospheric model. *J. geophys. Res.* **92**, 4649.

Kenner, R. D. and Ogryzlo, E. A. (1980) Deactivation of $O_2(A^3\Sigma_u^+)$ by O_2, O, and Ar. *Int. J. Chem. Kinetics* **12**, 501.

Kenner, R. D. and Ogryzlo, E. A. (1983) Rate constant for the deactivation of $O_2(A^3\Sigma_u^+)$ by N_2. *Chem. Phys. Lett.* **103**, 209.

Kenner, R. D. and Ogryzlo, E. A. (1984) Quenching of $O_2(A_{v=2} \rightarrow X_{v=5})$ Herzberg I band by O_2(a) and O. *Can. J. Phys.* **62**, 1599.

Kita, K., Higuchi, T. and T. Ogawa, T. (1989) Bayesian statistical inference of airglow profiles from rocket observational data: comparison with conventional methods. *Planet. Space Sci.* **37**, 1327.

Llewellyn, E. J. (1988) The concentration of atomic oxygen in the mesosphere and the thermosphere. *Planet. Space Sci.* **36**, 892.

Lopez-Moreno, J. J., Rodrigo, R. and Vidal, V. (1985) Radiative contamination in rocket-borne infrared photometric measurements. *J. geophys. Res.* **90**, 6617.

McDade, I. C., Llewellyn, E. J., Greer, R. G. H. and Murtagh, D. P. (1982) The altitude dependence of the $O_2(A^3\Sigma_u^+)$ vibrational distribution in the terrestrial nightglow. *Planet. Space Sci.* **30**, 1133.

McDade, I. C., Llewellyn, E. J., Greer, R. G. H. and Witt, G. (1984) Altitude dependence of the vibrational distribution of $O_2(c^1\Sigma_u^-)$ in the nightglow and the possible effects of vibrational excitation in the formation of $O(^1S)$. *Can. J. Phys.* **62**, 780.

McDade, I. C., Murtagh, D. P., Greer, R. G. H., Dickinson, P. H. G., Witt, G., Stegman, E. J., Llewellyn, E. J., Thomas, L. and Jenkins, D. B. (1986a) ETON 2: quenching parameters for proposed precursors of $O_2(b^1\Sigma_g^+)$ and $O(^1S)$ in the terrestrial nightglow. *Planet. Space Sci.* **34**, 789.

McDade, I. C., Llewellyn, E. J., Greer, R. G. H. and Murtagh, D. P. (1986b) ETON 3: altitude profiles of the nightglow continuum at green and near infrared wavelengths. *Planet. Space Sci.* **34**, 801.

McDade, I. C., Llewellyn, E. J., Murtagh, D. P. and Greer, R. G. H. (1987a) ETON 5: simultaneous rocket measurements of the OH Meinel $\Delta v = 2$ sequence and (8,3) band emission profiles in the nightglow. *Planet. Space Sci.* **35**, 1137.

McDade, I. C., Llewellyn, E. J., Greer, R. G. H. and Murtagh, D. P. (1987b) ETON 6: a rocket measurement of the O_2 infrared atmospheric (0–0) band in the nightglow. *Planet. Space Sci.* **35**, 1541.

Murtagh, D. P., Greer, R. G. H., McDade, I. C., Llewellyn, E. J. and Bantle, M. (1984) Representative volume emission profiles from rocket photometer data. *Ann. Geophys.* **2**, 467.

Murtagh, D. P., McDade, I. C., Greer, R. G. H., Stegman, J., Witt, G. and Llewellyn, E. J. (1986) ETON 4: an experimental investigation of the altitude dependence of the $O_2(A^3\Sigma_u^+)$ vibrational populations in the nightglow. *Planet. Space Sci.* **34**, 811.

Murtagh, D. P., Witt, G., Stegman, J., McDade, I. C., Llewellyn, E. J., Harris, F. and Greer, R. G. H. (1990) An assessment of proposed $O(^1S)$ and $O_2(b^1\Sigma_g^+)$ nightglow parameters. *Planet. Space Sci.* **38**, 43.

Offerman, D., Friedrich, V., Ross, P. and von Zahn, U. (1981) Neutral gas composition measurements between 80 and 120 km. *Planet. Space Sci.* **29**, 747.

Ogry, A. E. (1987) MSIS-86 thermospheric model. *J. geophys. Res.* **92**, 4649.

Rusch, D. W. and Sharp, W. E. (1981) Nitric oxide delta band emission in the Earth's atmosphere: comparison of a measurement and a theory. *J. geophys. Res.* **86**, 10, 111.

Sharp, W. E. (1985) Upper limits to [O] in the lower thermosphere from airglow. *Planet. Space Sci.* **33**, 571.

Sharp, W. E. (1991) The measurement of atomic oxygen in the mesosphere and thermosphere. *Planet Space Sci.* **39**, 617.

Sharp, W. E. and Kita, D. (1987) *In situ* measurement of atomic hydrogen in the upper mesosphere. *J. geophys. Res.* **92**, 4319.

Sharp, W. E. and Siskind, D. E. (1989) Atomic emission in the ultraviolet nightglow. *Geophys. Res. Lett.* **16**, 1453.

Siskind, D. E. and Sharp, W. E. (1990) A vibrational analysis of the $O_2(A^3\Sigma_u^+)$ Herzberg I system using rocket data. *Planet. Space Sci.* **38**, 1399.

Stegman, J. and Murtagh, D. P. (1988) High resolution spectroscopy of oxygen u.v. airglow. *Planet. Space Sci.* **36**, 927.

Stegman, J. and Murtagh, D. P. (1991) The molecular oxygen band systems in the u.v. nightglow: measured and modelled. *Planet. Space Sci.* **39**, 595.

Stegman, J., Murtagh, D. P. and Witt, G. (1989) Spectral composition of oxygen u.v. nightglow. *Trans Am. geophys. Un. EOS* **70**, 1238.

Thomas, L., Greer, R. G. H. and Dickinson, P. H. G. (1979) The excitation of the 557.7 nm line and Herzberg bands in the nightglow. *Planet. Space Sci.* **27**, 925.

Thomas, R. J. (1981) Analysis of atomic oxygen, the green line and Herzberg bands in the lower thermosphere. *J. geophys. Res.* **86**, 206.

Thomas, R. J. and Young, R. A. (1981) Measurement of atomic oxygen and related airglows in the lower thermosphere. *J. geophys. Res.* **86**, 7389.

Wasser, B. and Donahue, T. M. (1979) Atomic oxygen between 80 and 120 km: evidence for a latitudinal variation in vertical transport near the mesopause. *J. geophys. Res.* **84**, 1297.

Witt, G., Rose, J. and Llewellyn, E. J. (1981) The airglow continuum at high latitudes: an estimate of the NO concentration. *J. geophys. Res.* **86**, 623.

Witt, G., Stegman, J., Murtagh, D. P., McDade, I. C., Greer, R. G. H., Dickinson, P. H. G. and Jenkins, D. B. (1984) Collisional energy transfer and the excitation of $O_2(b^1\Sigma_g^+)$ in the atmosphere. *J. Photochem.* **28**, 365.

APPENDIX

The differentiation of a measured column emission rate to produce a volume emission rate (VER) introduces an uncertainty due to the amplification of noise in the measured profile. To assess this error, we have performed a large number of cyclic calculations. These consist of calculating the VER from the data using Fourier filtering techniques, integrating the profile, adding random noise and recalculating a new VER. After each cycle, the VER will, in general, be different from the previous one due to the randomness of the introduced noise. After 200 such cycles, a family of VERs is obtained. For each altitude one can then generate a histogram of points which reflect the distribution about some "best" value. Our error bars in Figs 2b, 3b and 4 are the one sigma deviations determined from these histograms. For example, in the Herzberg calculation we found that out of 200 calculations, about 70% of the derived peak emission values lay between 14 and 20, thus leading to an 18% error estimate for the peak value (see Fig. 3b). A similar error was found for the 7620 Å emission. At 100 km, this increases to about 30%. Of course, our error estimates are directly related to the amount of random noise that is added. The noise level was taken from the counting statistics for a 0.5 km bin at the bottom of the airglow layer. For both the Herzberg and atmospheric band, this was 10% of the signal. For the two green line profiles, the statistics were somewhat better; for Flight 1, the noise in the integrated intensity was about 4% while for Flight 2, it was about 2%. The resulting errors in the recovered VER are thus proportionally smaller than for the Herzberg and atmospheric band profiles. In addition, our estimate for the peak altitude for each emission feature is believed to be accurate to within ± 1 km.

These estimates are for random noise only; an additional systematic uncertainty is introduced by the filtering of high frequencies that may be actually present in the data. This is seen in the work of Murtagh *et al.* (1984) when they compared the VER recovered using Fourier filtering with their initial profile. The effect is to "round off" sharp peaks in the VER. It is also seen in Fig. 3b where the VER obtained using Fourier filtering is compared against that obtained using the linear least-squares fitting technique. This is more difficult to quantify since it depends upon the degree of filtering used which is itself somewhat subjective. Since our conclusions do not depend upon the existence of small-scale structure in our VER profiles (with the possible exception of the "bump" at 99–101 km which is shown to be independent of the analysis technique in Fig. 3b), the practical effect of this uncertainty is likely to be negligible.